

Cation Vacancy in Wide Bandgap III-Nitrides as Single-Photon Emitter: A First-Principles Investigation

Hang Zang, Xiaojuan Sun, Ke Jiang, Yang Chen, Shanli Zhang, Jianwei Ben, Yuping Jia, Tong Wu, Zhiming Shi,* and Dabing Li*

Single-photon sources based on solid-state material are desirable in quantum technologies. However, suitable platforms for single-photon emission are currently limited. Herein, a theoretical approach to design a single-photon emitter based on defects in solid-state material is proposed. Through group theory analysis and hybrid density functional theory calculation, the charge-neutral cation vacancy in III-V compounds is found to satisfy a unique 5-electron-8-orbital electronic configuration with T_d symmetry, which is possible for single-photon emission. Furthermore, it is confirmed that this type of single-photon emitter only exists in wide bandgap III-nitrides among all the III-V compounds. The corresponding photon energy in GaN, AlN, and AlGaIn lies within the optimal range for transfer in optical fiber, thereby render the charge-neutral cation vacancy in wide-bandgap III-nitrides as a promising single-photon emitter for quantum information applications.

color centers^[8,9] with atom-like isolated levels are promising types of single-photon sources due to the convenient combination with advanced technologies of the semiconductor industry. The color center, which is a kind of fluorescent defect in solid-state material with the wavefunction localized on the atomic scale length,^[10] can potentially realize single-photon emission at room temperature.^[11] For instance, the diamond's NV ($N_C V_C$) center,^[12] SiV ($Si_C V_C$) center;^[13] the silicon carbide's silicon-vacancy (V_{Si}) center,^[14] divacancy ($V_{Si} V_C$) center,^[15] antisite-carbon-vacancy ($C_{Si} V_C$) center;^[16] and the zinc oxide's zinc-vacancy (V_{Zn}) center^[17] have received a lot of investigations.

In recent years, benefits from the mature technique of material growth and device fabrication, III-V compounds have become commercial semiconductors,^[18] among them the III-nitrides that possess wide-bandgap^[19] meet the criteria of host material for single-photon emission. In 2017, Berhane et al. had realized the room-temperature single-photon emission in GaN.^[20] In 2018, Zhou et al. had reported near-infrared emitters based on GaN with high photon purity.^[21] In 2020, Xue et al. and Bishop et al. had reported room-temperature single-photon emission in AlN,^[22,23] the antisite-nitrogen-vacancy ($N_{Al} V_N$) and divacancy ($V_{Al} V_N$) were predicted to be possible sources of the single-photon signal.^[22] As the III-nitrides belong to ionic semiconductor, the dangling bond energy level lies in the lower part of the bandgap for cation vacancy (V_{cation}), while it lies in the upper part of the bandgap for anion vacancy (V_{anion}).^[24] It was found that the defect energy level for nitrogen-vacancy (V_N) in AlN was close to the conduction band maximum (CBM). Transition metal dopant substitution^[25] and strain-driven^[26] strategies were proposed theoretically to adjust the defect electronic configuration to make V_N in AlN suitable for single-photon emission. For V_{cation} , since its defect energy level was found close to the valence band maximum (VBM), many theoretical investigations were focused on negatively charged V_{cation} , including its light emission^[27–29] and carrier doping^[30] property. However, whether V_{cation} can realize single-photon emission by tuning its electronic configuration remains unclear.

By reviewing the previous reports, we find most of the successful host materials are in wurtzite and zinc-blende structures, in which all atoms are tetrahedrally coordinated. The four sp^3 dangling bonds (ψ_i , ($i = 1, 2, 3, 4$)) around a vacancy have

1. Introduction

Single-photon is suitable to serve as a quantum bit (qubit)^[1] for the encoding, communication, and measurement of quantum information^[2] since it can travel over long distances while interacting weakly with the environment and can be manipulated with linear optics.^[3] Single-photon emitter (SPE) is hence the central building block for many quantum information technologies. The early-stage SPE was based on single-atom,^[4,5] however, it suffered from drawbacks such as low efficiency and reliability. Solid-state materials including quantum dots^[6,7] and

Dr. H. Zang, Prof. X. Sun, Dr. K. Jiang, Dr. Y. Chen, S. Zhang, Dr. J. Ben, Dr. Y. Jia, T. Wu, Prof. Z. Shi, Prof. D. Li
State Key Laboratory of Luminescence and Applications, Changchun Institute of Optics, Fine Mechanics and Physics
Chinese Academy of Sciences
Changchun 130033, China
E-mail: shizm@ciomp.ac.cn; lidb@ciomp.ac.cn

Prof. D. Li
Center of Materials Science and Optoelectronics Engineering
University of Chinese Academy of Sciences
Beijing 100049, China

 The ORCID identification number(s) for the author(s) of this article can be found under <https://doi.org/10.1002/adv.202100100>

© 2021 The Authors. Advanced Science published by Wiley-VCH GmbH. This is an open access article under the terms of the Creative Commons Attribution License, which permits use, distribution and reproduction in any medium, provided the original work is properly cited.

DOI: 10.1002/adv.202100100

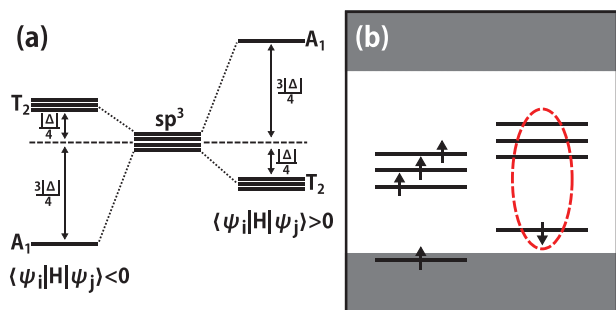


Figure 1. a) The schematic process of sp^3 dangling bond energy level splitting under T_d symmetry. b) The 5-electron-8-orbital electronic configuration when $\langle \psi_i | H | \psi_j \rangle < 0$.

the same energy level $\langle \psi_i | H | \psi_i \rangle = E$ and inter-bond interaction $\langle \psi_i | H | \psi_j \rangle = -\Delta/4$. Due to the interaction between dangling bonds, the energy level splits into a nondegenerate A_1 state and a triple degenerate T_2 state with an energy difference of Δ under the T_d symmetry. The relative position of A_1 and T_2 depends on the sign of $\langle \psi_i | H | \psi_j \rangle$ as shown in **Figure 1**, and it determines the relative energy level for different electronic configurations. For the case of $\langle \psi_i | H | \psi_j \rangle < 0$, the many-electron effect analysis shows that a ‘5-electron-8-orbital’ electronic configuration is suitable for single-photon emission. Whereas all the defect levels in the spin-up channel are occupied; in the spin-down channel, only the low energy A_1 level is occupied, and all the T_2 levels are empty, the optical emission corresponds to the transition of $A_1 \leftrightarrow T_2$ (details are described in the Supporting Information).

In this work, based on group theory analysis and first-principles computation, we present a comprehensive study of the single-photon emission property of V_{cation} in III-V compounds. We find that the charge-neutral V_{cation} in III-V compounds can meet the specific 5-electron-8-orbital electronic configuration. Moreover, the charge-neutral V_{cation} in wide bandgap III-nitrides including GaN, AlN, AlGaIn, and low In component InGaIn are thermodynamically stable and can serve as SPE. The corresponding defect energy level, formation energy, and photon energy of the proposed SPE are presented

2. Experimental Section

It was first characterized whether charge-neutral V_{cation} in III-V (III = Al, Ga, In; V = N, P, As) compounds satisfy the 5-electron-8-orbital electronic configuration. The band structures calculated with HSE06 hybrid functional are shown in **Figure 2** (the atomic structures are shown in Figure S3, Supporting Information). Taking the Fermi level as a reference, the VBM position of the host material tends to increase as the group III component varies from Al to In when fixing the group V component or as the group V component varies from N to As when fixing the group III component. The orbital contribution of anions around V_{cation} shows the defect levels of V_{cation} in the spin-up channel are fully occupied, while in the spin-down channel the A_1 state lies below the T_2 states and only the A_1 state is occupied. This indicates a negative inter-bond interaction ($\langle \psi_i | H | \psi_j \rangle$) between the anion dangling bonds, the charge-neutral V_{cation} in III-V compounds thus satisfies the 5-electron-8-orbital electronic configuration.

To serve as an SPE, the defect energy level of V_{cation} should lie within the bandgap to make the optical transition do not introduce interference from electronic states of the host material.^[24] The relative position between the defect energy level of V_{cation} and band edge of host material depends on the energy level of the anion sp^3 dangling bond, the corresponding symmetry-induced splitting, and the bandgap of the host material. For V_{cation} in III-phosphide and III-arsenide, as shown in Figure 2d–i, the T_2 states in the spin-down channel are located within the bandgap, while the A_1 state lies below the VBM, this can be attributed to the low sp^3 level of P/As atom. Because the T_2 states are degenerate and are all unoccupied, the charge-neutral V_{cation} in III-phosphide or III-arsenide is not suitable for single-photon emission. Since the sp^3 dangling bond energy of the N atom is the highest one among all the group V elements,^[31] the possible case that the A_1 level lies above VBM should be III-nitride. As shown in Figure 2a–c, for V_{cation} in AlN, GaN, and InN, the A_1 level in the spin-down channel lies above the VBM. However, the bandgap of InN is too narrow, the defect levels of V_{cation} are all above the CBM. While V_{cation} in wide bandgap III-nitrides of GaN and AlN are suitable for single-photon emission whereas all the A_1 and T_2 levels lie within the bandgap.

Based on our previous analysis, it has been proposed to use charge-neutral V_{cation} in wide bandgap III-nitride as a potential SPE. To numerically assess the single-photon emission property, the defect level of V_{cation} in larger supercells of GaN and AlN was calculated, each includes 399 atoms as shown in **Figure 3a₁,e₁**, with a Γ point only K -mesh sampling. The defect level diagrams of V_{cation} in GaN and AlN are shown in Figure 3a₂,e₂. The energy splitting (Δ) between A_1 and T_2 in GaN (1.45 eV) is smaller to that in AlN (1.64 eV). The interatomic distance (see Table S2, Supporting Information) shows that the distance between the N atom around V_{cation} is smaller in AlN, which results in a larger inter-bond interaction and thereby larger energy splitting (Δ) in AlN. The energy differences between defect level and VBM/CBM in GaN and AlN are all larger than 0.9 eV, indicating the thermal transition from the host material to the defect state is small.

The strain effect on the III-nitrides epilayer, which can be achieved by mechanical wafer bending experimentally, has been widely investigated. Here the strain effect on the single-photon emission property of V_{cation} in GaN and AlN was also studied, biaxial strain vertical to the (0001) direction including a 95% compress strain and a 105% tensile strain was considered. The results (see Figure S9, Supporting Information) indicate that for V_{cation} in GaN and AlN, both the band edge position of the host material and the defect energy level change under the extrinsic strain, and they are all located within the bandgap in the considered strain range. For specific, the bandgap of the host material and the energy difference between A_1 and T_2 increase when applying a compress strain, while they decrease when applying a tensile strain. This offers a way to tune the single-photon emission property of V_{cation} experimentally.

To examine whether the proposed SPE is optically active, the absorption spectrum of V_{cation} was calculated, the results for V_{cation} in GaN and AlN are shown in Figure 3a₃,e₃, respectively. Since there are no in-gap states in the spin-up channel and the T_2 states are nearly degenerate in the spin-down channel, the obvious peak below 2 eV corresponds to the transition from A_1 to T_2 , this indicates an optical transition can occur between the two

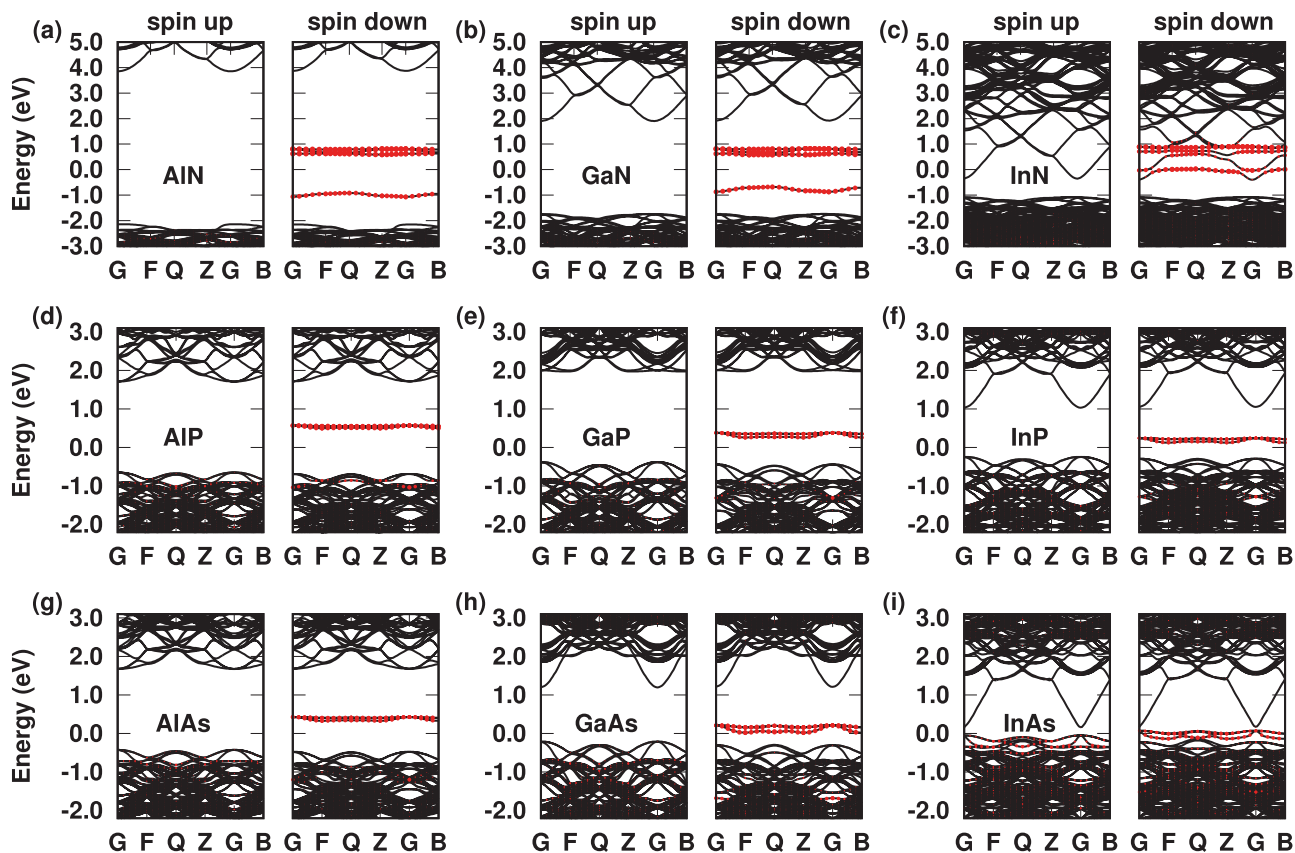


Figure 2. Band structures for neutral V_{cation} in III-V compounds calculated with HSE06 functional, here G (0.0, 0.0, 0.0), F (0.0, 0.5, 0.0), Q (0.0, 0.5, 0.5), Z (0.0, 0.0, 0.5), B (0.5, 0.0, 0.0) refer to the high-symmetry special points in the first Brillouin zone, the Fermi level is set to zero, the orbital contribution of four anions around V_{cation} is represented by red dots.

states. The small and broad absorption of V_{cation} in AlN in Figure 3e₃ includes the transition from VBM to T_2 and from A_1 to CBM, the calculated moment matrix $|\langle \psi_i | p | \psi_j \rangle|^2$ (see Equation S24, Supporting Information) shows that the corresponding magnitude of $A_1 \leftrightarrow T_2$ is about 3 times larger than VBM $\leftrightarrow T_2$ and $A_1 \leftrightarrow \text{CBM}$, thus the broad absorption has little effect on the single-photon emission property. The absorption spectrum for V_{cation} in strained GaN and AlN are shown in Figure S9, Supporting Information, the corresponding absorption peak of V_{cation} blue (red) shifted under a compress (tensile) strain, consistent with the change of the energy difference between A_1 and T_2 .

In addition to the binary GaN and AlN, III-nitride alloy is also widely investigated since it has a tunable bandgap. The single-photon emission property of V_{cation} in III-nitride alloy is now calculated, the wurtzite structure of III-nitride alloy is built by cluster expansion method,^[32] the corresponding unit cell structures are shown in Figure S1, Supporting Information. The structure of V_{cation} in III-nitride alloy is determined by directly remove a cation from the perfect alloy, as indicated later, the formation energy of neutral V_{cation} is high, such a non-equilibrium way is practical to generate V_{cation} in the experimental condition.

For AlGa_xN alloy as a host material, the atomic structures with low, medium, and high Al composition of 0.25, 0.5, and 0.8 are chosen as representatives. The calculated band structures indicate that the CBM of AlGa_xN is contributed by the s orbital of

the N atom (see Figure S2, Supporting Information). The VBM of AlGa_xN with low Al composition is contributed by the p_x and p_y orbital of the N atom. For AlGa_xN with high Al composition, the VBM is mainly contributed by the p_z orbital of the N atom. This results in a different light emission mode in the electrically pumped light emission device,^[33] this property can be used to separate the light signals from host material and V_{cation} efficiently. The calculated defect energy level and absorption spectrum of V_{Al} in AlGa_xN with different Al compositions are shown in Figure 3b–d (the results for V_{Ga} in AlGa_xN are shown in Figure S10, Supporting Information), the qualitative property of defect levels of V_{cation} in AlGa_xN is the same as that of GaN and AlN. Due to the different interactions between the Al–N and Ga–N bond, the N atoms around V_{cation} move unsymmetrically from their original position. Such a symmetry-lowering effect caused by the random alloy reduces the coupling between sp^3 dangling bonds and splits the degenerated T_2 states. Also, as shown in Figure 3, the optical transition is allowed between A_1 and T_2 for V_{cation} in AlGa_xN, the moment matrix (see Equations S19 and S21, Supporting Information) of the broad absorption peak in Figure 3c₃,d₃ is similar to the case of V_{cation} in AlN, and it does not affect the single-photon emission property.

For InGa_xN alloy, previous calculation showed that V_{cation} was suitable for single-photon emission in GaN but not InN, which is due to the low CBM position of InN. Since the bandgap of InGa_xN

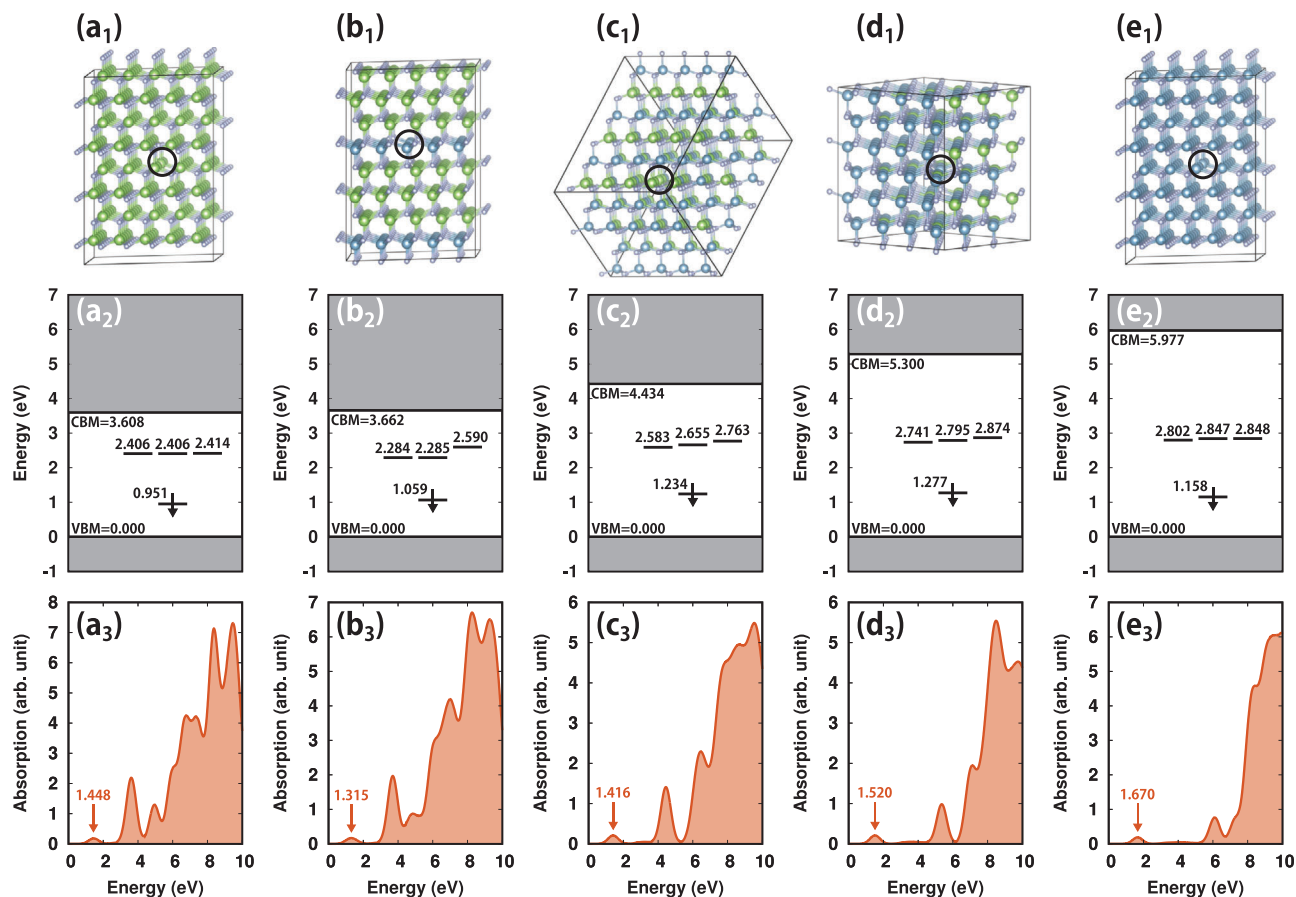


Figure 3. a₁–e₁) The atomic supercell structures for V_{Ga} in GaN, and V_{Al} in Al_{0.25}Ga_{0.75}N, Al_{0.5}Ga_{0.5}N, Al_{0.8}Ga_{0.2}N, and AlN, the corresponding defect energy levels in the spin-down channel (the VBM is set to zero) and absorption spectrum for calculated with HSE06 functional are shown in (a₂–e₂) and (a₃–e₃), respectively.

decreases monotonically with the In component, there should be a maximum In component for V_{cation} to serve as an SPE in In-GaN alloy. Therefore, the effect of different In compositions on the single-photon emission property of V_{cation} is calculated, it is found that for V_{cation} in In_{0.25}Ga_{0.75}N, the lowest T₂ state of V_{cation} is nearly in resonance with the CBM, in this case, the insulation of the CBM is broken. While for a low In component case of In_{0.125}Ga_{0.875}N, all the defect energy levels in the spin-down channel are located within the bandgap (see Figures S4 and S6, Supporting Information). It was concluded that for V_{cation} to realize single-photon emission in InGaN, a maximum component of In should not exceed about 25%. The calculated defect level and absorption spectrum of V_{cation} in In_{0.125}Ga_{0.875}N are qualitatively the same as the case of GaN and AlN, the results are shown in Figure S8, Supporting Information.

To quantitatively characterize the single-photon emission property of V_{cation}, the zero-phonon line (ZPL) was calculated, which is the optical transition energy without the phonon contribution. The excited-state structure was optimized with a constraint DFT method^[34] by restricting the excited-state electronic configuration. The results are listed in Table 1, and the corresponding interatomic distances between anions at ground (excited) state are listed in Table S2, Supporting Information. It can be seen that the ZPL of V_{cation} in pure GaN and AlN shows

a monotonic dependence on the strain, it increases (decreases) under the compress (tensile) strain. For AlGaN alloy, though the mixing of Al has a similar monotonic effect on the lattice constant, the local environment for V_{cation} differs a lot, it affects the geometry of ground and excited states and then affects the ZPL. Even in the same AlGaN alloy, the ZPL of V_{Al} and V_{Ga} differs a lot, thus, the ZPL does not show an obvious dependence on the mixing ratio of AlGaN. In recent experimental investigations, the single-photon emission in GaN with ZPL from 1085 to 1340 nm has been observed,^[21] based on our ZPL results, the V_{cation} should have contributions to the corresponding single-photon signal. The ZPL of V_{cation} in these III-nitrides has a large overlap with the optimal range of ≈1.2–1.6 μm that can reduce the attenuation^[35] for optical fiber telecommunication. Besides, the calculated radiative lifetime τ_{rad} of V_{cation}, as listed in Table 1, are comparable to that of the NV⁻ center in diamond (≈10–30 ns).^[36] These advantages indicate that V_{cation} is suitable for practical quantum communication application.

As one of the key factors for the proposed SPE, the 5-electron-8-orbital electronic configuration should be stable in experimental conditions. Here, the thermodynamic stability of V_{cation} in GaN, AlN, and AlGaN/InGaN alloy was assessed. The formation energies as a function of the Fermi level are shown in Figure 4. It is seen that different charge states of

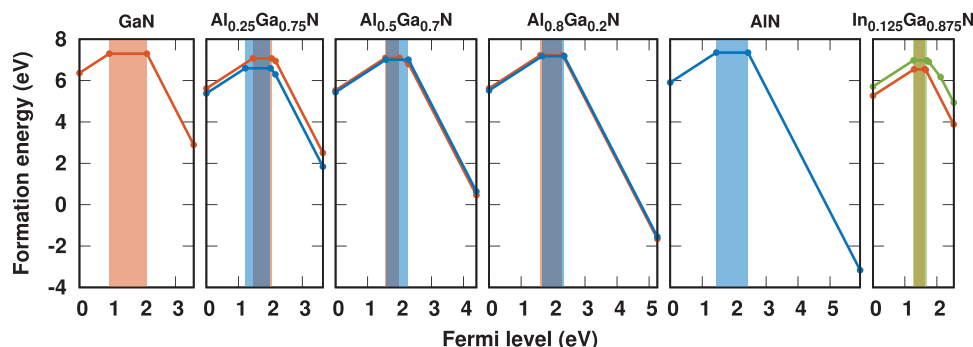


Figure 4. The formation energy of V_{cation} in GaN, AlN, AlGa, and InGa at N rich condition, the red, blue, and green lines corresponds to V_{Ga} , V_{Al} , and V_{In} , respectively, the corresponding colored area indicates the Fermi level where neutral V_{cation} is stable.

Table 1. Calculated moment matrix $|\langle \psi_i | p | \psi_j \rangle|^2$, transition energy ΔE between defect levels, radiative lifetime τ_{rad} , and ZPL for V_{cation} in GaN, AlN, AlGa, and InGa.

	$ \langle \psi_i p \psi_j \rangle ^2$ [au]	ΔE [eV]	τ_{rad} [ns]	ZPL [eV]
V_{Ga} in 95% strain-GaN	1.90×10^{-2}	1.97	14.23	1.49
V_{Ga} in GaN	1.05×10^{-2}	1.45	35.18	0.70
V_{Ga} in 105% strain-GaN	6.06×10^{-3}	1.08	81.56	0.57
V_{Al} in $\text{Al}_{0.25}\text{Ga}_{0.75}\text{N}$	9.22×10^{-3}	1.22	48.59	0.68
V_{Ga} in $\text{Al}_{0.25}\text{Ga}_{0.75}\text{N}$	1.31×10^{-2}	1.30	32.04	0.92
V_{Al} in $\text{Al}_{0.5}\text{Ga}_{0.5}\text{N}$	1.61×10^{-2}	1.35	25.80	0.76
V_{Ga} in $\text{Al}_{0.5}\text{Ga}_{0.5}\text{N}$	1.31×10^{-2}	1.25	34.28	0.70
V_{Al} in $\text{Al}_{0.8}\text{Ga}_{0.2}\text{N}$	1.60×10^{-2}	1.46	24.72	0.84
V_{Ga} in $\text{Al}_{0.8}\text{Ga}_{0.2}\text{N}$	1.71×10^{-2}	1.45	23.29	0.96
V_{Al} in 95% strain-AlN	2.59×10^{-2}	2.10	10.83	1.96
V_{Al} in AlN	2.24×10^{-2}	1.64	16.03	0.94
V_{Al} in 105% strain-AlN	8.54×10^{-3}	1.36	50.63	0.72
V_{In} in $\text{In}_{0.125}\text{Ga}_{0.875}\text{N}$	7.38×10^{-3}	1.14	62.78	0.62
V_{Ga} in $\text{In}_{0.125}\text{Ga}_{0.875}\text{N}$	4.48×10^{-3}	1.17	100.63	0.56

V_{cation} defect can be stable in the bandgap, the neutral V_{cation} is stable in the lower part in the bandgap, indicating the p-type III-nitrides is requested to guarantee the 5-electron-8-orbital configuration. Recently, through using superlattice doping,^[37] polarization-induced doping^[38] techniques, etc., the p-type doping efficiency in III-nitrides can be effectively enhanced, it is possible to take advantage of these carrier doping techniques to make charge-neutral V_{cation} thermodynamically stable. However, as an impurity, the dopant may affect the property of SPE, the effect of $\text{Mg}_{\text{cation}}$ as an example was tested, the results show the major property of SPE will not be affected by the cation dopant as long as the structure and local electronic configuration of V_{cation} is maintained (see Figures S5 and S7, Supporting Information). For practical application, since the atomic structure of V_{cation} is simple, there are various techniques to achieve it such as electron irradiation,^[39] and pulse laser irradiation,^[40] the SPE based on V_{cation} is thus achievable in experimental conditions.

For the SPE in bulk material, refraction is an issue that strongly influences the signal extracting. In practice, recent structures of III-nitrides generally have a size of less than a few hundred

nanometers, which is far less than the photon wavelength, the refraction issue is thus irrelevant. Since the mono vacancy structure possesses no inversion symmetry, the external field induces charge fluctuation and causes spectral diffusion,^[41] however, its magnitude is not necessarily large for a single vacancy as indicated in a recent theoretical study.^[42] The reported SPE here is only applicable in GaN and AlN among all the III-V compounds, where the inter-bond interaction $\langle \psi_i | H | \psi_j \rangle$ is negative, and the A_1 state lies below T_2 . As indicated in Figure 1, when $\langle \psi_i | H | \psi_j \rangle > 0$ the T_2 states lies below A_1 , which results in a different electronic configuration, further numerical calculations of vacancy with a T_d symmetry in other material is a promising way to searching new SPE.

3. Conclusion

In summary, we have symmetrically investigated the single-photon emission property of V_{cation} in the III-V compound. Based on the group theory analysis and first-principles calculation with hybrid density functional, we predict that the charge-neutral V_{cation} in III-V compounds has a unique 5-electron-8-orbital electronic configuration, which is suitable for single-photon emission. Furthermore, we confirm that the charge-neutral V_{cation} can only serve as SPE in wide bandgap III-nitrides among all the III-V (III = Al, Ga, In; V = N, P, As) compounds. The charge-neutral V_{cation} in AlN, GaN, and III-nitride alloy is thermodynamically stable and the corresponding ZPL lies within the optimal range for low-loss fiber transmission, which makes this type of SPE particularly useful in practical applications. Our investigation also sheds light on the concept of designing an SPE with a precisely tuned electronic configuration.

Supporting Information

Supporting Information is available from the Wiley Online Library or from the author.

Acknowledgements

This work was supported by the National Science Fund for Distinguished Young Scholars (61725403), the National Natural Science Foundation

of China (61922078, 61804152, 61874118, 61834008, and 12004378), the Special Fund for Research on National Major Research Instruments (61827813), the Key Research Program of Frontier Sciences, Chinese Academy of Sciences (CAS) (Grant No. ZDBS-LY-JSC026), Key Research Program of CAS (Grant No. XDPB22), the Youth Innovation Promotion Association of CAS, and the CAS Talents Program.

Conflict of Interest

The authors declare no conflict of interest.

Data Availability Statement

Research data are not shared.

Keywords

AlGaIn, cation vacancy, density functional theory, group theory, single-photon emitters

Received: January 12, 2021
Revised: May 9, 2021
Published online: July 26, 2021

- [1] B. Lounis, M. Orrit, *Rep. Prog. Phys.* **2005**, *68*, 1129.
- [2] F. Xu, X. Ma, Q. Zhang, H.-K. Lo, J.-W. Pan, *Rev. Mod. Phys.* **2020**, *92*, 025002.
- [3] M. D. Eisaman, J. Fan, A. Migdall, S. V. Polyakov, *Rev. Sci. Instrum.* **2011**, *82*, 071101.
- [4] F. De Martini, G. Di Giuseppe, M. Marrocco, *Phys. Rev. Lett.* **1996**, *76*, 900.
- [5] A. Kuhn, M. Hennrich, G. Rempe, *Phys. Rev. Lett.* **2002**, *89*, 4.
- [6] S. Kako, C. Santori, K. Hoshino, S. Götzinger, Y. Yamamoto, Y. Arakawa, *Nat. Mater.* **2006**, *5*, 887.
- [7] X. Sun, P. Wang, T. Wang, L. Chen, Z. Chen, K. Gao, T. Aoki, M. Li, J. Zhang, T. Schulz, M. Albrecht, W. Ge, Y. Arakawa, B. Shen, M. Holmes, X. Wang, *Light Sci. Appl.* **2020**, *9*, 159.
- [8] V. A. Norman, S. Majety, Z. Wang, W. H. Casey, N. Curro, M. Radulaski, *InfoMat* **2020**, <https://doi.org/10.1002/inf2.12128>.
- [9] G. Zhang, Y. Cheng, J.-P. Chou, A. Gali, *Appl. Phys. Rev.* **2020**, *7*, 031308.
- [10] C. E. Dreyer, A. Alkauskas, J. L. Lyons, A. Janotti, C. G. Van de Walle, *Annu. Rev. Mater. Res.* **2018**, *48*, 1.
- [11] I. Aharonovich, D. Englund, M. Toth, *Nat. Photonics* **2016**, *10*, 631.
- [12] C. Kurtziefer, S. Mayer, P. Zarda, H. Weinfurter, *Phys. Rev. Lett.* **2000**, *85*, 290.
- [13] J. P. Goss, R. Jones, S. J. Breuer, P. R. Briddon, S. Öberg, *Phys. Rev. Lett.* **1996**, *77*, 3041.
- [14] M. Widmann, S.-Y. Lee, T. Rendler, N. T. Son, H. Fedder, S. Paik, L.-P. Yang, N. Zhao, S. Yang, I. Booker, A. Denisenko, M. Jamali, S. A. Mo-menzadeh, I. Gerhardt, T. Ohshima, A. Gali, E. Janzén, J. Wrachtrup, *Nat. Mater.* **2015**, *14*, 164.
- [15] W. F. Koehl, B. B. Buckley, F. J. Heremans, G. Calusine, D. D. Awschalom, *Nature* **2011**, *479*, 84.
- [16] S. Stelletto, B. C. Johnson, V. Ivády, N. Stavrias, T. Umeda, A. Gali, T. Ohshima, *Nat. Mater.* **2014**, *13*, 151.
- [17] A. J. Morfa, B. C. Gibson, M. Karg, T. J. Karle, A. D. Greentree, P. Mulvaney, S. Tomljenovic-Hanic, *Nano Lett.* **2012**, *12*, 949.
- [18] A. L. Greenaway, J. W. Boucher, S. Z. Oener, C. J. Funch, S. W. Boettcher, *ACS Energy Lett.* **2017**, *2*, 2270.
- [19] D. Li, K. Jiang, X. Sun, C. Guo, *Adv. Opt. Photonics* **2018**, *10*, 43.
- [20] A. M. Berhane, K.-Y. Jeong, Z. Bodrog, S. Fiedler, T. Schröder, N. V. Triviño, T. Palacios, A. Gali, M. Toth, D. Englund, I. Aharonovich, *Adv. Mater.* **2017**, *29*, 1605092.
- [21] Y. Zhou, Z. Wang, A. Rasmita, S. Kim, A. Berhane, Z. Bodrog, G. Adamo, A. Gali, I. Aharonovich, W.-b. Gao, *Sci. Adv.* **2018**, *4*, eaar3580.
- [22] Y. Xue, H. Wang, N. Xie, Q. Yang, F. Xu, B. Shen, J.-j. Shi, D. Jiang, X. Dou, T. Yu, B.-q. Sun, *J. Phys. Chem. Lett.* **2020**, *11*, 2689.
- [23] S. G. Bishop, J. P. Hadden, F. D. Alzahrani, R. Hekmati, D. L. Huffaker, W. W. Langbein, A. J. Bennett, *ACS Photonics* **2020**, *7*, 1636.
- [24] J. R. Weber, W. F. Koehl, J. B. Varley, A. Janotti, B. B. Buckley, C. G. Van de Walle, D. D. Awschalom, *Proc. Natl. Acad. Sci. U. S. A.* **2010**, *107*, 8513.
- [25] J. B. Varley, A. Janotti, C. G. Van de Walle, *Phys. Rev. B* **2016**, *93*, 161201.
- [26] H. Seo, M. Govoni, G. Galli, *Sci. Rep.* **2016**, *6*, 20803.
- [27] J. Neugebauer, C. G. Van de Walle, *Appl. Phys. Lett.* **1996**, *69*, 503.
- [28] K. B. Nam, M. L. Nakarmi, J. Y. Lin, H. X. Jiang, *Appl. Phys. Lett.* **2005**, *86*, 222108.
- [29] N. Nepal, M. L. Nakarmi, J. Y. Lin, H. X. Jiang, *Appl. Phys. Lett.* **2006**, *89*, 092107.
- [30] S. B. Zhang, S.-H. Wei, A. Zunger, *Phys. Rev. Lett.* **2000**, *84*, 1232.
- [31] M. Lannoo, J. Bourgoin, *Point Defects in Semiconductors I, Springer Series in Solid-State Sciences*, Vol. 22, Springer, Berlin, Heidelberg **1981**.
- [32] J. Sanchez, F. Ducastelle, D. Gratias, *Physica A* **1984**, *128*, 334.
- [33] C. Reich, M. Guttman, M. Feneberg, T. Wernicke, F. Mehnke, C. Kuhn, J. Rass, M. Lapeyrade, S. Einfeldt, A. Knauer, V. Kueller, M. Weyers, R. Goldhahn, M. Kneissl, *Appl. Phys. Lett.* **2015**, *107*, 142101.
- [34] A. Gali, E. Janzén, P. Deák, G. Kresse, E. Kaxiras, *Phys. Rev. Lett.* **2009**, *103*, 186404.
- [35] G. Wolfowicz, F. J. Heremans, C. P. Anderson, S. Kanai, H. Seo, A. Gali, G. Galli, D. D. Awschalom, *arXiv:2010.16395* **2020**.
- [36] X. Zhou, Z. Zhang, W. Guo, *Nano Lett.* **2020**, *20*, 4136.
- [37] E. F. Schubert, W. Grieshaber, I. D. Goepfert, *Appl. Phys. Lett.* **1996**, *69*, 3737.
- [38] J. Simon, V. Protasenko, C. Lian, H. Xing, D. Jena, *Science* **2010**, *327*, 60.
- [39] C. A. McLellan, B. A. Myers, S. Kraemer, K. Ohno, D. D. Awschalom, A. C. Bleszynski Jayich, *Nano Lett.* **2016**, *16*, 2450.
- [40] T. Kurita, N. Mineyuki, Y. Shimotsuma, M. Fujiwara, N. Mizuochi, M. Shimizu, K. Miura, *Appl. Phys. Lett.* **2018**, *113*, 211102.
- [41] A. Sipahigil, K. D. Jahnke, L. J. Rogers, T. Teraji, J. Isoya, A. S. Zibrov, F. Jelezko, M. D. Lukin, *Phys. Rev. Lett.* **2014**, *113*, 113602.
- [42] P. Udvarhelyi, R. Nagy, F. Kaiser, S.-Y. Lee, J. Wrachtrup, A. Gali, *Phys. Rev. Appl.* **2019**, *11*, 044022.